Colloid Polym Sci (2002) 280: 599–606
DOI 10.1007/s00396-001-0642-3

ORIGINAL CONTRIBUTION

Hirofumi Okabayashi
Makoto Ishida
Haruhiro Yuki
Norikatsu Hattori
Hideki Masuda
Charmian J. O'Connor

Phase structures of the *N*-acetyl-L-glutamic acid oligomeric benzyl esters (exact residue numbers 4, 6, 8, and 12)–dioxane systems and their optical properties

Received: 29 August 2001
Accepted: 20 November 2001
Published online: 8 May 2002

H. Okabayashi (✉) · M. Ishida
H. Yuki · N. Hattori · H. Masuda
Department of Applied Chemistry,
Nagoya Institute of Technology,
Gokiso-cho, Showa-ku,
Nagoya 466-8555, Japan

C.J. O'Connor
Department of Chemistry, The University of Auckland, Private Bag 92019, Auckland, New Zealand

Abstract A series of *N*-acetyl-L-glutamic acid oligomeric benzyl esters with exact residue numbers (4, 6, 8, 10, and 12) has been synthesized by a stepwise procedure.

It has been found that the phase maps of these oligomer-dioxane systems consist of three regions (I : an isotropic solution, II : a liquid crystalline phase, and III : a two-phase (I and II) solution). In particular, for the samples with residue numbers 6, 8, and 12, selective light scattering of coloured regions in the transparent II and III (bottom-layer) regions have been investigated by the use of UV-visible absorption spectra, leading to the conclusion that there exists a helical axis in the structure of the supramolecular aggregates formed by these oligomeric molecules.

Introduction

Elliot and Ambrose [1] first discovered that high-molecular-weight poly-γ-benzyl-L-glutamate (PBLG) takes up an α-helical conformation even in organic solutions, as well as in the solid state, and that a liquid crystalline structure is formed in concentrated solutions. A cholesteric liquid crystalline structure of PBLG solutions has also been identified by Robinson et al. [2, 3, 4].

For low-molecular-weight PBLG, a β-sheet-structure has been assumed by Blout and Asadourian [5], and has been studied in detail by analysis of the infrared band characteristics of the amide group, which is sensitive to the conformation of a polypeptide [6, 7, 8, 9, 10, 11]. Imae et al. [12] identified the formation of an anisotropic phase in solutions of low-molecular-weight PBLG.

The intramolecular hydrogen bonding in the α-helix provides PBLG-molecules with considerable rigidity, which allows them to be regarded as rod-like. This rigidity is an important factor in the physico-chemical properties of the liquid crystals [13], since it provides molecular ordering in the liquid-crystalline state. Thus, for more than 40 years, PBLG solutions in the liquid crystalline state have been utilized as an excellent model for research into the phase behavior of rigid polymers, and a tremendous number of research investigations has been undertaken. In particular, the relevance to industrial application of the physico-chemical properties, including the rheological and optical properties of PBLG, has been investigated by Aoki, White and Fellers [14], Kiss and Porter [15], and Dadmum and Han [16].

Concentrated solutions of oligopeptides also provide an interesting class of lyotropic liquid crystals. In particular, the molecular structures of γ-benzyl-L-glutamate oligomers with an average degree of polymerization in organic solvents, have been investigated by use of viscometric and infrared spectroscopic methods [17]. The aggregate structure formed by γ-benzyl-L-glutamate oligomers (residue number $N_p = 4$ and 6) in organic solvents has been discussed [18, 19, 20, 21, 22]. For these oligomeric molecules, the aggregate structure in concentrated solutions still remains unresolved and its further investigation is highly desirable.

In our previous paper [23], we have used infrared and SANS spectral analysis to demonstrate that a series of *N*-acetyl-L-glutamic acid oligomeric benzyl esters (AN_pZ), with exact residue numbers ($N_p = 4$, 6, 8, and 12, not-averaged over the degree of polymerization, synthesized by a stepwise procedure), form supramolecular aggregates in dioxane, in which antiparallel β-sheet structures, preferentially-stabilized by self-assembly through intermolecular hydrogen bonding, are one-dimensionally stacked. Such an aggregational structure should be reflected in the physico-chemical properties of the oligomer–dioxane binary system.

In this present study, a series of *N*-acetyl-L-glutamic acid oligomeric benzyl esters was utilized to examine the phase behaviors of the AN_pZ–dioxane systems and their optical properties in connection with the supramolecular aggregates formed by each AN_pZ oligomeric molecule.

Experimental

Materials

N-Acetyl-L-glutamic acid oligomeric benzyl esters (AN_pZ, N_p = residue number, $CH_3CO[NHCH(CH_2CH_2CO_2\text{-benzyl})CO]_{N_p}O$-benzyl),

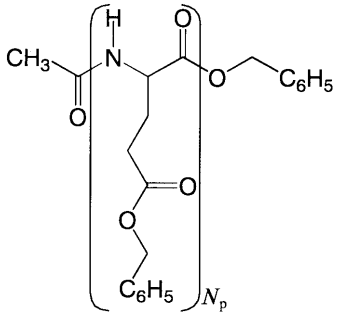

with exact residue numbers (4, 6, 8, and 12), were prepared by the stepwise procedure described previously [24].

The oligomers thus prepared were recrystallized in dichloromethane-petroleum ether. The samples (residue number, $N_p = 4$ and 6) were identified by elemental analysis. The agreement between the calculated and observed values for each atom of these samples was within 0.3%. For the samples with residue number $N_p = 8$ and 12, identification was made by ^{1}H NMR.

The residue numbers (N_p) of the AN_pZ series used for the present study were 4, 6, 8, and 12 (abbreviations: A4Z, A6Z, A8Z, and A12Z, respectively).

Phase map determination

Sample solutions were prepared by weighing the AN_pZ oligomer and dioxane into glass ampoules and the contents were sealed and homogenized by shaking. The temperature dependence of the phase features of the samples was observed by visual inspection as they were held in a temperature-controlled water-bath (rate of temperature elevation and cooling: 0.1 °C min^{-1}). A polarizing microscope (Olympus-pos) with a temperature-variable hot stage was also used to confirm the phase features.

Light-scattering measurements and critical aggregation concentration determination

Light-scattering measurements were carried out on a Union Giken DLS 700 light-scattering photometer using He-Ne laser light (5 mW) at 632.8 nm. The refractive index increment of the sample solutions was measured on the Union Giken RM-102 differential refractometer at 633 nm. The temperature was kept at 298.5 ± 0.3 K by circulating temperature-controlled water through the cell housings. The reduced intensity (R_Θ) of light scattered at an angle Θ from a sample solution (concentration, C in g cm^{-3}) is given by the following equation:

$$R_\Theta = R_\Theta^0 + KMP(\Theta)(C - C_0) \quad (1)$$

when the external interference is negligible. In this equation, R_Θ^0, M, and $P(\Theta)$ are the reduced intensity at the critical aggregation concentration (C_0), the apparent weight-average molecular weight, and the particle scattering factor, respectively; K is the optical constant:

$$K = 4\pi^2 n_0^2 (\partial n/\partial c)_c^2 \Big/ L_A \lambda^4 \quad (2)$$

where n_0 and $(\partial n/\partial c)_c$ are the refractive index of solvent and the reflexive index increment of solution, respectively, measured at wavelength λ, and L_A is Avogadro's constant.

The critical aggregation concentration (CAC) of the solute in dioxane and the molecular weight of the aggregate were determined from plots of R_{90} vs concentration for samples of $N_p = 6$ where $R^0{}_{90}$ is the reduced scattering intensity.

X-Ray powder diffraction pattern and infrared absorption measurements

X-Ray powder diffraction patterns were obtained by use of an RAD-RC diffractometer with counter-monochromator (CuL_α, 50 kV, 110 mA). Infrared absorption spectra were recorded on a Perkin-Elmer 1600 Fourier-transform infrared (FTIR) spectrometer (4000–400 cm^{-1}) with the sample dispersed in KBr discs for the solid states and with the sample-dioxane solution sandwiched between two CaF_2-plate windows (spacer 0.015 mm).

Refractive index measurements

Refractive indices (n_e and n_o) of the AN_pZ–dioxane solutions were measured by use of an Abbe refractometer 2 T (Atago Co., Ltd) temperature-controlled at 298 K, utilizing the 589 nm ordinary and extraordinary ray.

UV-visible spectral measurements

Bragg-scattering spectra of the samples in the visible region were measured with an angle of incidence equal to 1800 using a Hitachi U-3500 spectrometer with a deuterium discharge tube and iodine-tungsten lump. The sample solutions were placed in a 10.0 nm-quartz cell with a cell-holder thermostatted at 298 ± 0.04 K. Bragg-scattering spectra for an angle of incidence of 90° were measured, using a multi-channel spectrometer Fastevert S-2600 (350–1050 nm) with a Fluorescence measurement unit (740,120) at room temperature.

Results

The X-ray powder diffraction patterns were measured for the AN_pZ oligomers in the solid state. Lattice

spacings, coming from the distance between β-sheet type peptide chains and the side-chain spacing, were observed in common at 4.71–4.74 Å and 15.53–15.85 Å [17], providing ample evidence that the series of AN_pZ oligomers (N_p = 4, 6, 8, and 12) take up a β-sheet structure in the solid state.

The FTIR spectra for a series of AN_pZ oligomers in the solid state have also been measured at room temperature and compared with those of simple amide molecules [8, 9] and PBLG [10]. The amide I bands were observed in common at 1685–1705 cm^{-1} and 1615–1637 cm^{-1}, respectively, and were regarded as characteristic bands of the antiparallel-type β-sheet structure.

In this present study, for the AN_pZ–dioxane binary systems, the residue number (N_p)-dependence on phase behavior has been focused on the structural reorganization aggregates formed by the AN_pZ oligomeric molecules in dioxane.

Phase behaviors of the AN_pZ oligomer–dioxane systems

Phase maps of the AN_pZ oligomers (N_p = 4, 6, 8, and 12)–dioxane systems are shown in Fig. 1. The phase maps consist of three regions (I, II, and III). A homogeneous and transparent one-phase solution was obtained in region I, and a homogeneous, turbid or transparent and viscous one-phase solution was obtained in region II. In region III, a two-phase solution with a transparent upper layer and a turbid (or transparent) and viscous bottom layer was obtained. It has been confirmed for this region III that the upper layer is optically isotopic and that the bottom layer is in a liquid crystalline state. The volume percentage of the upper layer in region III decreased linearly and, conversely, that of the bottom layer increased with increasing weight-percentage of the sample. This observation is a consequence of the Lever rule and proves that the region III system is in an equilibrium state between the upper and bottom layers.

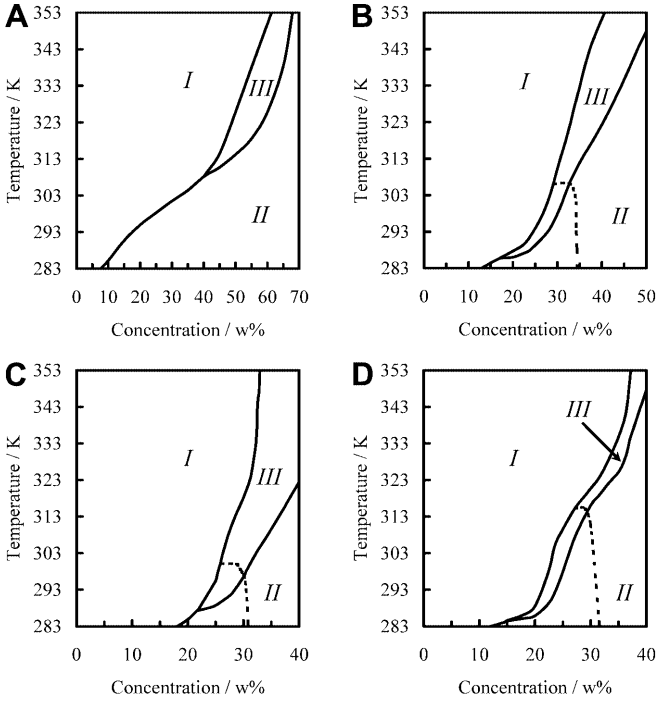

Fig. 1. Phase maps of the AN_pZ–dioxane systems **A** A4Z–dioxane, **B** A6Z–dioxane, **C** A8Z–dioxane, and **D** A12Z–dioxane). The region surrounded by a *broken line* shows the colored region

For the phase maps of A4Z, it has been found that a two-phase solution (region III) exists in the concentrated region above 40 w% and in the higher temperature region above 35 °C. As a consequence of visual inspection, we have confirmed that the coloured region does not exist in region II (turbid) in the ranges of temperature and concentration used in the present study.

For the phase map of A6Z, we emphasize that the transparent colored regions (II and III (bottom-layer)) appear below 308 K and that the colour strongly depends upon the concentration: green (27 w%), blue (30 w%), dark blue (32 w%) and below 27 w% the colour changes to red or yellow.

For A8Z, in the transparent II and III (bottom-layer) regions, mainly purple-coloured regions appeared at concentrations below 32 w% and at a temperature less than 303 K.

For A12Z, transparent and purple-coloured regions appeared in the concentration range 26–32 w% at 318 K, but below 26 w% the colour changed to red or yellow, depending upon the concentration and temperature.

For the AN_pZ series (N_p = 4, 6, 8, and 12), light scattering from dioxane solutions in region I has been measured at various concentrations. Since no angular dependence of the light scattering was found for the sample solutions in Region I, the molecular weight of the aggregate was determined from the Debye plots for the 90° direction. The apparent weight-average molecular weights (M) and aggregation numbers (m) of the oligomeric aggregates are listed in Table 1, together with the critical aggregation concentrations (CAC) at which formation of an aggregate occurs.

Table 1. Apparent weight-average molecular weight (M) and aggregation number (m) of the AN_pZ-oligomers

AN_pZ	CAC	Molecular weight	Aggregation number
	w%	M	m
N_p = 4	> 5		
N_p = 6	0.48	3.682×10^4	25
N_p = 8	< 0.1	4.404×10^4	23
N_p = 12	< 0.1	5.761×10^4	21

The infrared absorption spectra (in particular, in the amides I and II-mode region) were examined at various AN_pZ-concentrations for region I, which exists in common in the phase maps of the AN_pZ–dioxane system. The results showed that self-assembly of the chiral AN_pZ systems, which aggregate through intermolecular hydrogen bonding, brings about the conformational conversion from the β-turn to the antiparallel β-sheet structure (to be reported separately).

For the coloured II and III (bottom layer) regions, which were observed under irradiation by white light, the colour of the species depends not only upon the concentration but also the angle of incidence, the angle of visual inspection and the temperature, implying that the optical properties are caused by selective light scattering (that is, Bragg-like scattering) arising from the liquid crystalline structures. This phenomenon has previously been observed with cholesterol and its related compounds [25], which scatter light to give a variable iridescent color depending upon substance-temperature and angle of incident beam. Therefore, the optical properties of these AN_pZ–dioxane samples seem to be analogous to those of a cholesteric liquid crystal.

Birefringence of the AN_pZ–dioxane systems

The refractive indices (n_e and n_o) of the AN_pZ (N_p = 4, 6, 8, and 12)–dioxane systems have been examined using the extraordinary and ordinary ray, in order to characterize the phase structures of regions I, II, and III. The n_e and n_o values for representative sample solutions are listed in Table 2, and the concentration-dependence of the n_e and n_o values for the A6Z–dioxane and A12Z–dioxane systems are shown in Fig. 2A and B.

For the A6Z–dioxane sample in region II and for the A12Z–dioxane sample in regions II and III (bottom layer), we note that the birefringence values

Table 2. Refractive index of AN_pZ–dioxane systems at 298 K

Sample	Phase	C (w%)	n_o[a]	n_e[b]	Δn[c]
A4Z	I	20	1.447	1.447	0.000
A6Z	I	20	1.446	1.446	0.000
	II	35	1.464	1.467	0.003
	II	40	1.471	1.475	0.004
	III[d]	27	1.458	1.458	0.000
A8Z	I	15	1.439	1.439	0.000
	II	40	1.472	1.476	0.004
	III[d]	28	1.456	1.456	0.000
A12Z	I	20	1.451	1.451	0.000
	II	28	1.454	1.456	0.002
	II	40	1.468	1.472	0.004
	III[d]	24	1.452	1.453	0.001

[a] *R*efractive index measured by use of ordinary ray
[b] *R*efractive index measured by use of extraordinary ray
[c] Birefringence $\Delta n = n_e - n_o$
[d] Bottom layer

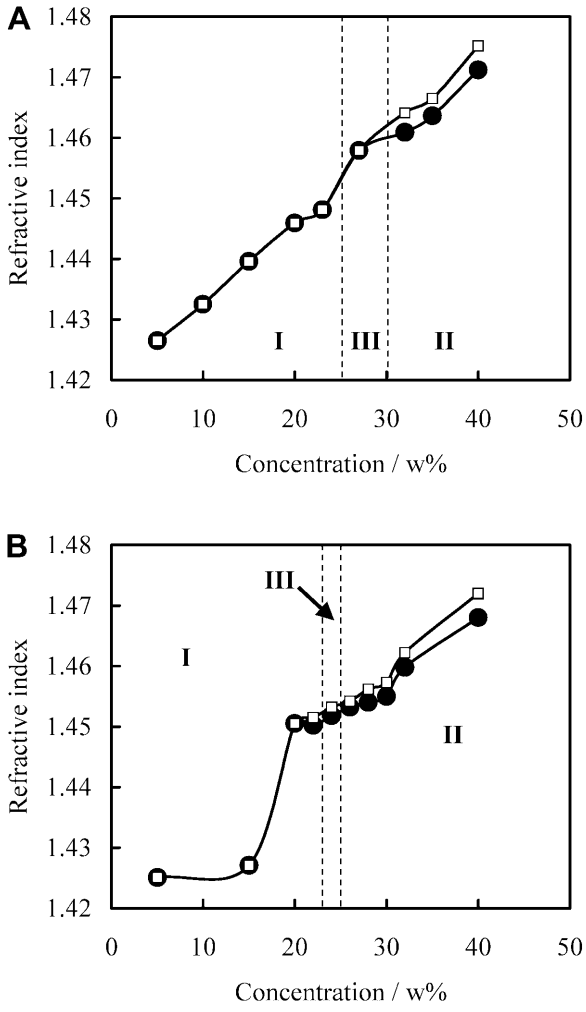

Fig. 2. Refractive index of the **A** A6Z–dioxane and **B** A12Z–dioxane solutions measured at 298 K (● n_o and □ n_e)

(Δn) are positive ($n_e > n_o$) and become larger with an increase in concentration, indicating that the sample solutions are optically positive. We may assume that region II (or III (bottom layer)) in the AN_pZ (N_p = 6 and 12)–dioxane systems is similar to a nematic mesophase, since the Δn_e value of a nematic liquid crystal (for example, *p*-azoxyanisole) is generally positive ($n_e > n_o$) [25]. In the nematic mesophase, rod-like molecules are aligned along the long axis of the molecule, but they do not form a layered structure analogous to that of a smectic mesophase. That is, they are irregular in the direction perpendicular to the long axis of the molecule.

For the A12Z–dioxane system in region I, the refractive index rapidly increases with an increase in concentration above 15 w% until it finally comes close to the values observed in region III (bottom layer), indicating that micro phase separation may occur in the concentrated region I.

Optical properties of the AN_pZ–dioxane systems and their highly ordered structures

In order to understand the highly ordered structures of the AN_pZ-aggregates, their selective light scattering (Bragg-like scattering) [26, 27] has been investigated by use of the UV-visible-absorption spectra of the samples in the 300–800 nm region. The focus has been on the A6Z–dioxane system, which provides a relatively strong intensity compared with those for the other sample systems (A8Z–dioxane and A12Z–dioxane systems).

Figure 3 shows the UV-visible absorption spectra of the A6Z–dioxane systems measured at various concentrations. For the A6Z–dioxane samples (10 and 25 w%) in the isotropic solution (Region I), only the absorption band at 257.5 nm, derived from the π–π^* electronic transition of the benzyl groups, appeared in the UV region (spectra not shown). We have confirmed that these sample solutions absorbed no measurable radiation in the visible portion of the spectrum. However, for the sample solutions (27, 29, 31, 32, and 35 w%) in the coloured regions, the selective light-scattering maximum characteristics of the cholesteric liquid crystal were observed in the visible region. We can regard them as Bragg-scattering spectra, which were measured at an angle of incidence of 180° by use of a visible light absorption spectrometer. The selective scattering maximum evidently shifts to a shorter-wavelength with an increase in concentration and finally disappears in the visible-light region (300–650 nm) for the sample solutions in the more highly concentrated region above 40 w%. The disappearance of this maximum may come about from a shifting of the scattering maximum to a shorter wavelength below 300 nm. Selective light scattering maxima, which were observed for the A6Z–dioxane samples, are not as sharp as those seen in the mixed cholesteric liquid crystal [25], probably because of the polydispersity of the aggregates formed by A6Z molecules.

For the A6Z (32 w%)–dioxane solution, the Bragg-like scattering spectrum, which was measured for a 90 ° angle of incidence, is shown in Fig. 4 a. In addition to a predominant scattering maximum at 474 nm, other maxima at 386, 412, 558, 626, and 700 nm are observed, although their intensities are small compared with that of the 474 nm maximum, a result that again indicates polydispersity of the aggregates.

Therefore, the optical properties of the A6Z oligomeric solutions imply that the aggregates of the oligomers formed in these concentrated solutions provide Bragg-like scattering arising from local order with an internal helical axis, similar to that proposed for the cholesteric liquid crystal [25].

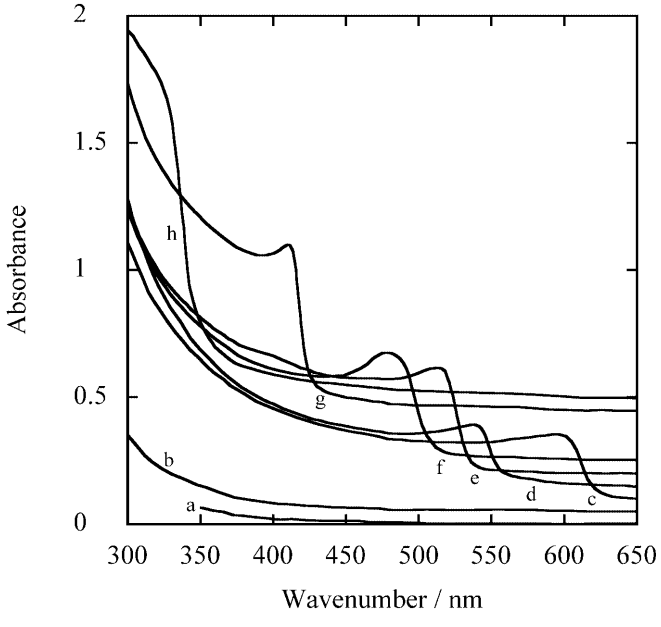

Fig. 3. Absorption spectra of the A6Z–dioxane solutions in the 300–650 nm region: 10 w% (**a**), 25 w% (**b**), 27 w% (**c**), 29 w% (**d**), 31 w% (**e**), 32 w% (**f**), 35 w% (**g**), and 40 w% (**h**)

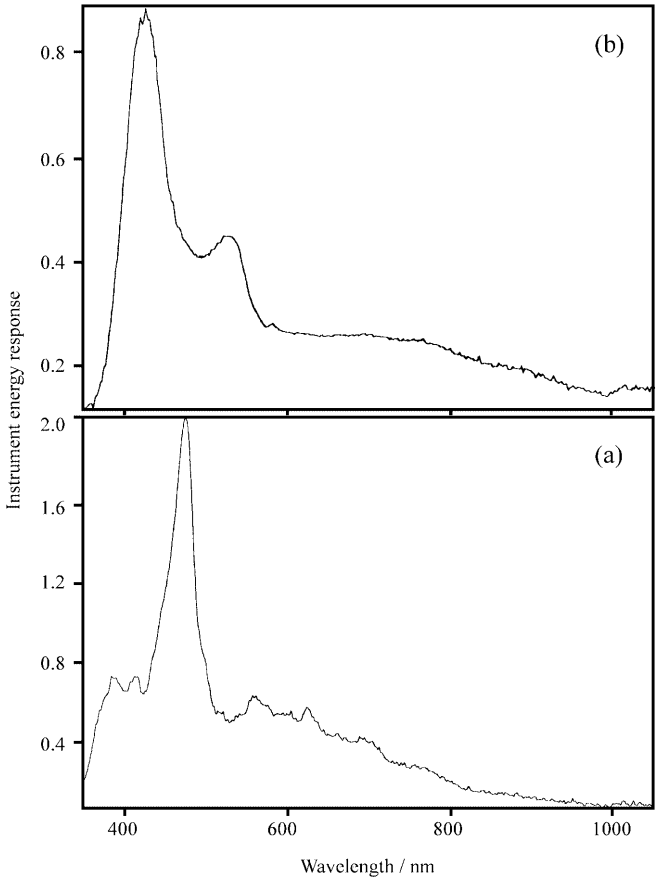

Fig. 4. Selective light-scattering spectra of the **a** A6Z (32 w%)–dioxane and **b** A12Z (28 w%)–dioxane solutions measured for a 90° angle of incidence

The selective light-scattering spectrum of the A12Z (28 w%)–dioxane solution, measured for a 90 ° angle of incidence, is shown in Fig. 4b. We note the existence of two selective scattering maxima (424 and 525 nm), implying that the two species of aggregates, which are different in their extent of local order, are predominantly present in this sample.

As Fergason has discussed in detail for various cholesteric materials [25], the helicoidal structures of cholesteric materials result in selective reflection of visible light within a band of wavelength of width $\Delta\lambda$ centered at a wave-length λ_0, such that:

$$\begin{aligned} \lambda_0 &= \bar{n} \cdot P \\ \Delta\lambda &= \Delta n \cdot P \end{aligned} \tag{3}$$

where P is the pitch of the helical structure, $\bar{n}$is the average refractive index and Δn is the birefringence of the medium. The angular dependence of the selectively reflected wavelength is approximately expressed as:

$$\lambda_\Theta = \frac{P_{\bar{n}}}{m}\cos\left[\frac{1}{2}\sin^{-1}\left(\frac{\sin\Theta_i}{\bar{n}/n}\right) + \frac{1}{2}\sin^{-1}\left(\frac{\sin\Theta_r}{\bar{n}/n}\right)\right] \tag{4}$$

where Θ_i and Θ_r are the angles of incidence and reflection, respectively. Therefore, when the incident beam is parallel to the helical axis, the selective scattering of visible light with the longest wavelength is observed, while with an incidence obviously oblique to the axis, selective scattering of visible light with a shorter wavelength occurs.

Thus, we may assume that the selective scattering maximum, with wave-length λ_0, which was observed for the AN_pZ–dioxane samples, comes from an incidence parallel to the helical axis, and the selective scattering with a wavelength, λ_Θ, shorter than λ_0, is derived from an incidence oblique to the axis. Thus, we can calculate the pitch of the helix from Eq. 1, since the wavelength of the scattering maximum is directly proportional to the pitch of the helical structure.

The concentration-dependence of the selective scattering maximum (λ_0) has been investigated for the A6Z–dioxane system, as shown in Fig. 5. It is evident that the maximum, λ_0, shifts linearly to a shorter wavelength with an increase in concentration, indicating that the concentration dependence of the pitch (P) can be expressed by $(\mathrm{d}P/\mathrm{d}C) < 0$.

Figure 6 shows the temperature dependence of the λ_0 value for the two A6Z–dioxane samples in the coloured region. For the less-concentrated sample (27 w%), the λ_0 value shifts to a markedly shorter wavelength above 298 K, while for the more concentrated sample (32 w%) variation of λ_0 occurs above 303 K, although the variation is not so marked. Such a difference in the temperature dependence of λ_0 between the two samples may be ascribed to the following

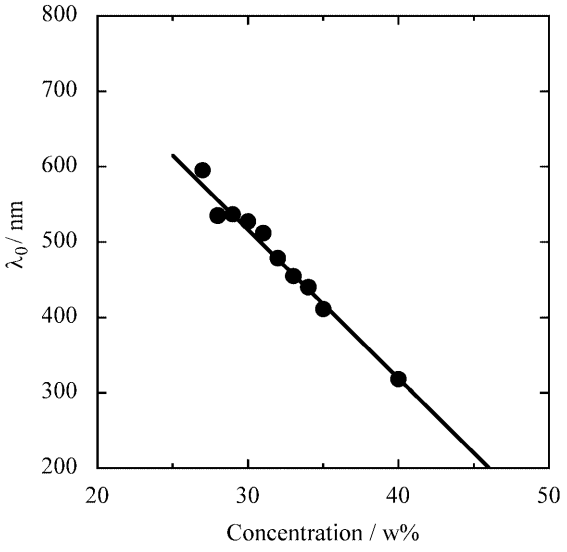

Fig. 5. Concentration dependence of selective scattering maximum for the A6Z–dioxane system

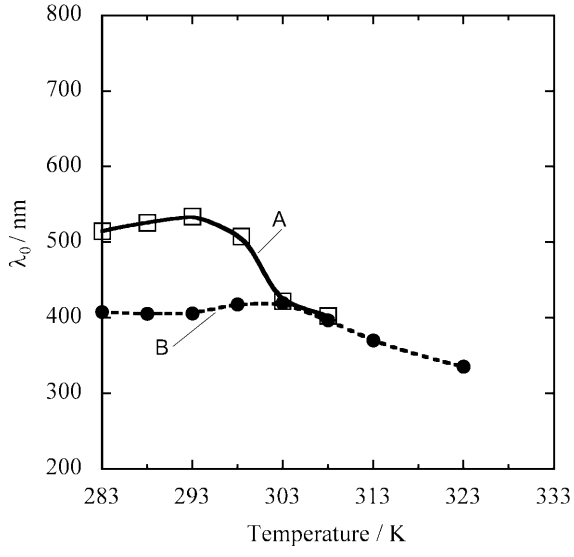

Fig. 6. Temperature dependence of the selective scattering maximum of the **A** A6Z (27 w%)–dioxane and **B** A6Z (34 w%)–dioxane samples

reason. For the less-concentrated (27 w%) sample, when the temperature rises from 283 K to 308 K, a phase transition from the liquid crystalline region II to the concentrated isotropic region I (through region III) occurs, leading to a marked variation in the extent of ordering in the aggregates. Conversely, for the concentrated (32 w%) sample, an increase in temperature from 283 K to 323 K induces a transition from the liquid crystalline region II to the liquid crystalline phase III (bottom layer), in which the difference in the

extent of local ordering in the aggregates between the two phases must be small.

Thus, the concentration and temperature-dependence of the λ_0 value reveal that the pitch of the helical axis in the local order of the aggregate may change, depending upon the concentration and the temperature. That is, an increase in concentration makes the pitch shorter, due to structural variation in the aggregate (for example, an increase in aggregation number and variation in shape). A rise in temperature brings about a structural variation in the aggregate induced by the phase transition, leading to a change of pitch.

When we use the refractive index measured in this present study, we can evaluate the pitch from Eq. 3. For example, using the refractive index and selective scattering maximum for the 32 w% A6Z–dioxane sample of 1.465 and 475 nm, respectively, leads to a pitch value of 324 nm.

In the very concentrated region, in which the selective light-scattering maximum disappears, the pitch of this helical axis probably becomes shorter.

Thus, the selective scattering maximum, observed for the A6Z–dioxane and A12Z–dioxane samples in region II, indicates that a helical axis exists in the structure of the highly ordered aggregates formed by these molecules.

Discussion

We may now assume that the iridescent color of the AN_pZ–dioxane systems, which strongly depends upon concentration and temperature, reflects the highly ordered structures of the aggregates.

IR and SANS measurements were therefore carried out on the dioxane solutions of the AN_pZ-oligomer aggregates in region I [23], in order to elucidate their microstructures. Results of special relevance to this present study show that the antiparallel β-sheet oligomeric molecule may be regarded as a flat molecule which is one-dimensionally stacked to form the rod-like aggregate and that the aggregates are in a poly-dispersed state. The average aggregation number (N_n) and number-average molecular weight (M_n) for these oligomeric aggregates are $N_n = 18$, $M_n = 2.6\times10^4$, $\alpha kT = 30$ kJ/mol for A6Z (2.3×10^{-2} mol/l), $N_n = 27$, $M_n = 5.1\times10^4$ $\alpha kT = 33$ kJ/mol for A8Z (1.6×10^{-2} mol/l), and $N_n = 19$, $M_n = 5.3\times10^4$ $\alpha kT = 32$ kJ/mol for A12Z (1.2×10^{-2} mol/l), indicating that the N_n and M_n values strongly depend upon the residue number. For A4Z, the intensities of the SAXS spectra of the A4Z–dioxane system even at a concentration of 30 w%, were too weak for analysis, indicating that there are no aggregates detectable by SAXS at such a concentration. However, from the IR spectral results of the AN_pZ–dioxane solutions, we may assume that formation of A4Z aggregates is possible in concentrated solutions (above 30 w%). Thus, we may regard these aggregates as supramolecular aggregates. The difference in the aggregational structures during the different AN_pZ-oligomer systems should be reflected in the physico-chemical properties.

For the chiral AN_pZ–dioxane systems in regions II and III (bottom layer), it may be assumed that a mature rod-like aggregate, in which the antiparallel β-type AN_pZ molecules are one-dimensionally stacked through hydrogen bonds, involves the helical axis in the structure. However, this assumption does not imply that the rod-like aggregate takes up a helical structure. Probably, this helical axis (that is, the origin of iridescence color) comes from fluctuations of the *N* and *C*-terminal and their vicinal residues of the oligopeptides and of β-sheet disk molecule at their vicinal areas of rod-like aggregate. The fluctuations may be caused by the difference in hydrogen-bond energy between *N* and *C*-terminal residues or that between both terminal and central portions of an aggregate.

In general, the two-terminal residues of an oligomeric molecule may be different in hydrogen bond environment from the residues sandwiched by both terminal residues [23]. Recently, we have examined the ^{1}H-NMR spectra of the AN_pZ–dioxane systems (to be submitted separately), indicating that the chemical shifts of the ^{1}H resonance peaks markedly reflect specific difference in hydrogen bond environment. Thus, we assume that the hydrogen bond energies of *N* and *C*-terminal residues in the β-sheet oligopeptide are smaller than those of the central portion.

Moreover, in our previous paper [23], for the SANS intensity spectra of the AN_pZ–dioxane systems, we have demonstrated that a rod like aggregation with smaller aggregation numbers provides smaller hydrogen bond energy (αkT). Furthermore, the more the β-sheet disk-like molecules comes close to both ends in a rod, the smaller becomes the hydrogen-bond energy between the disks. Such a difference in hydrogen-bond energy probably brings about the twisted structure in the hydrogen-bond network, leading to the appearance of a helical axis, which provides a selective light scattering maximum.

In cholesteric liquid crystals, which provide a strong negative birefringence and selective scattering, as proposed by de Vries [28], the structure is built up of a large number of thin birefringent layers, with the principal axes of the successive layers turned through a small angle. The helical arrangement of birefringent layers thus produced scatters the light to give an iridescent colour.

It is also well-known that in concentrated solutions, PBLG forms mesomorphic phases akin to cholesteric liquid crystals [2, 3, 4] and that the conformation in the mesomorphic phase has been identified as that of the α-helix [29]. In the mesomorphic phase of concentrated

PBLG solutions, the rod-like PBLG molecules with tight intramolecular hydrogen bonding are packed approximately parallel to each other, but with a small helical twist relative to one another about an axis perpendicular to the molecular axis. This twist may produce characteristic negative birefringence.

For the chiral AN_pZ–dioxane systems in regions II and III (bottom layer), we may assume that the mature rod-like aggregates with a helical axis are packed approximately parallel to each other. Thus, the structure may be regarded as a nematic arrangement, bringing about the positive birefringence. This assumption is strongly supported by our deuterium NMR results of the liquid crystalline phases for the same sample systems [30], which provide the conclusion that the structure of the liquid crystalline phase is similar to that in a nematic phase. That is, rod-like aggregates formed by the AN_pZ-oligomeric molecules may be aligned to the direction of the long axis of an aggregate but there may be irregularities in alignment in the direction perpendicular to the long axis.

Conclusion

For the dioxane solutions of *N*-acetyl–L–glutamic acid oligomeric benzyl esters with exact residue numbers (4, 6, 9, 14), phase diagrams have been examined. In particular, iridescent coloured regions have been found in the liquid crystalline phases. Selective light-scattering of the coloured regions have been examined by use of UV-visible spectroscopic method, leading to the conclusion that there exists a helical axis in the structure of supramolecular aggregates formed by these oligomeric molecules. The origin of the existence of a helical axis have been discussed in relation to the fluctuation of terminal residues or residues close to them arising from the difference in hydrogen-bond energy.

The chiral AN_pZ–dioxane systems in the liquid crystalline phase are optically positive, showing that these aggregates are in a molecular alignment similar to that which exists in the nematic mesophase. This formation is probably caused by variation of the molecular alignment in a supramolecular aggregate.

References

1. Elliott A, Ambrose EJ (1950) Disc Farad Soc 9:246
2. Robinson C (1956) Trans Farad Soc 52:571
3. Robinson C, Ward JC (1957) Nature 180:1183
4. Robinson C, Ward JC, Beevers RB (1958) Disc Farad Soc 25:29
5. Blout ER, Asadourian A (1956) J Am Chem Soc 78:955
6. Ambrose EJ, Elliott A (1950) Proc R Soc London Ser A 205:47
7. Elliott A (1954) Proc R Soc London Ser A 221:104
8. Miyazawa T, Shimanouchi T, Mizushima S (1956) J Chem Phys 24:408
9. Miyazawa T, Shimanouchi T, Mizushima S (1958) J Chem Phys 29:611
10. Miyazawa T, Blout ER (1961) J Am Chem Soc 83:712
11. Masuda Y, Miyazawa T (1967) Die Makromolekulare Chemie 103:261
12. Imae T, Ikeda S, Yamashita O, Ashida T (1981) Mol Cryst Liq Cryst 65:73
13. Cohen Y, Dagan A (1995) Macromolecules 28:7638
14. Aoki H, White JL, Fellers JF (1979) J Appl Polym Sci 23:2293
15. Kiss G, Porter RS (1980) J Polym Sci Polym Phys 18:361
16. Dadmum MD, Han CC (1994) Macromolecules 27:7522
17. Imae T, Ikeda S (1973) Biopolymers 12:1203
18. Okahashi K, Ikeda S (1979) Biopolymers 18:2105
19. Ikeda S, Okahashi K (1979) Biopolymers 18:2115
20. Imae T, Okahashi K, Ikeda S (1981) Biopolymers 20:2553
21. Imae T, Ikeda S (1984) Biopolymers 23:2573.
22. Imae T, Ikeda S (1985) Biopolymers 24:585
23. Ishida M, Takai M, Okabayashi H, Masuda H, Furusaka M, O'Connor CJ (2001) Phys Chem Chem Phys in press
24. Uehara T, Hirata H, Okabayashi H, Taga K, Yoshida T, Kojima H (1994) Colloid & Polymer Sci 272:692
25. Fergason JL (1966) Mol Cryst 1:293
26. Brown GH, Shaw WG (1957) Chem Rev 57:1049
27. Chandrasekhar S, Srinivasa Rao KN (1968) Acta Crystallogr A 24:445
28. de Vries H (1951) Acta Crystallogr 4:219
29. Parry DA, Elliott A (1965) Nature 206:616
30. Yoshino A, Ishida M, Yuki H, Okabayashi H, Masuda H, O'Connor CJ (2001) Colloid & Polym Sci, accepted